Supplemental Methods

Generation of chicken anti-human TRPV1 antibody

Affinity purified antibodies were generated by Aves Labs, Inc. (Tigard, OR) against a Keyhole limpet hemocyanin conjugate of the following peptide: KRTLSFSLRSSRVSGRHWKN, located within the C-terminal region of the human TRPV1 protein.

Cell sorting using Fluo4 and resiniferatoxin (RTX) activation to identify TRPV1+ embryonic DRG

DRGs were dissected from E16.5 embryonic rats (Sprague Dawley, Charles River Wilmington, MA) and dissociated using Liberase Blendzyme 3 (0.5 U/ml in HBSS, Roche Applied Science, Indianapolis, IL) for 1 hour. To determine if RTX-induced calcium influx is sustained long enough for cell sorting, ratiometric calcium imaging was performed on cultured DRG cells loaded with 2.5 μM Fura-2 AM (Molecular Probes, Eugene, OR) and stimulated with 200 nM RTX as described previously (1). Intracellular calcium remained elevated for >15 minutes (Figure 1A), long enough to perform fluorescence-activated cell sorting (FACS) based on this signal. Prior to FACS, DRG cells were loaded with 100 nM Fluo-4 AM (Molecular Probes) and TRPV1+ neurons were activated by addition of 200 nM resiniferatoxin (2). The dissociated cell preparation was also pre-labeled with Alexa Fluor 647-conjugated Isolectin IB4 (Invitrogen) and 1 μg/ml DAPI (Invitrogen) before sorting. FACS was performed using a MoFlo® Astrios cell sorter (Beckman Coulter, Brea, CA). Debris and dead cells were filtered out based on size and DAPI staining, respectively (Figure 1B). Baseline Fluo-4 intensity was recorded by sorting labelled unstimulated primary DRG neurons. This measurement was used as a

reference point for calcium influx after stimulation with RTX and further sorting was based on IB4 binding and calcium influx after RTX (Figure 1C). Cell sorting was performed using 18 psi for sheath fluid pressure, 0.5 psi differential between sheath fluid pressure and sample fluid pressure with a 100-micron nozzle. The pressure was selected to prevent lysis as cells exited the nozzle, which can occur at higher psi. An RNase inhibitor (recombinant from human placenta, New England BioLabs) was added to the sorting media to block degradation. Sorted cells were collected directly into TRIzol LS Reagent (Thermo Fisher Scientific).

Datasets for RNA-Seq analyses

Several RNA-Seq datasets were mined from the SRA database in FASTQ format and analyzed using the MAGIC pipeline. Human keratinocyte data were mined from BioProject PRJNA30709 (7 samples); Human skin samples were mined from BioProject PRJNA307599 (6 control samples) (3); Human placenta samples were mined from BioProject PRJNA308450 (19 samples) (4). Datasets generated for the present manuscript have also been deposited into the SRA database. The embryonic rat FACS sorting experiment (Supplemental Figure 1) is deposited under BioProject# PRJNA428250.

General care and behavioral assessments in rats

Male Sprague-Dawley rats (200-300g, Harlan Laboratories, Indianapolis, IN) were group housed according to standard procedures, and fed *ad libitum* except for fasting (12-15 hrs) prior to each orofacial operant testing session. As needed, rats were shaved under

isoflurane anesthesia (1-2.5%, inhalation) 1 day prior to testing. A model of orofacial inflammatory pain was used as previously described (5). Briefly, awake rats were gently restrained and carrageenan (6 mg in 150 µl PBS, Sigma-Aldrich) was injected subcutaneously into the mid-cheek region of the face bilaterally using a 25-gauge needle. Capsaicin cream (0.075%, Thomson Micromedex, CO) was also applied topically to produce nociceptive sensitization (6). Capsaicin cream was liberally applied to all of the shaved areas of the facial region of awake rats and left on for 5 min. The rats were gently restrained to prevent grooming or ingestion of capsaicin. The capsaicin was removed with a moist paper towel, and rats underwent operant testing immediately thereafter.

Supplemental methodology for peripheral delivery of RTX

A subset of rats (N = 2) was treated via a cut-down approach, where an incision was made in the midline of the head between the eyes. A small, freeing incision was made at the medial portion of the orbit and a small piece of Surgicel® (Johnson and Johnson) soaked in RTX (10 µl) or vehicle (10 µl) was placed directly onto the left or right ION within the same rat. This procedure was done to minimize retrograde spread of solution back towards the trigeminal ganglia (TG).

Systemic TRPV1 antagonism

We evaluated the effects of the TRPV1 antagonist AMG 9810 (Tocris Bioscience, Ellisville, MO). AMG 9810 (36 mg/kg, N=4) was dissolved in dimethyl sulfoxide (DMSO) and injected i.p. (750 µl). The control group (N=4) received 10% DMSO. Rats

were gently restrained for these injections and topical capsaicin was applied (5 min) and rats were tested on the operant system 30 minutes after AMG 9810 or vehicle injection.

Capsaicin eye wipe assay

The afferent function of the trigeminal nerve was evaluated using a capsaicin-induced eye wipe response, as described previously (8). Briefly, a 0.1% capsaicin solution (50 µl) was dropped onto the cornea of the eye, and the number of eye wipes was counted for 1 minute. Rats were tested at baseline prior to cisternal or infraorbital nerve injection of RTX or vehicle, then again at ≥ 1 week following injection.

Mechanical sensitivity measurement

Mechanical reflex sensitivity was assessed using an 'electronic von Frey' meter (IITC INC/ Life Sciences Instruments), as described previously (9). Rats were allowed to gently rest in one of the examiner's hands, and the filament was applied perpendicular to the skin over the body of the superficial masseter muscle, and a head withdrawal reaction was considered the endpoint response. This was repeated three times on each side of the face (every few seconds) in an alternating left-side then right-side fashion. The force that elicited a head withdrawal response was recorded and the mean was calculated for the session.

Operant orofacial thermal sensitivity

Pain sensitivity was assessed in the orofacial region using an operant thermal paradigm, as described previously (5, 7). The room temperature was maintained at 22 ± 1°C for all behavioral tests. Briefly, testing was performed in an acrylic cage with a 4 x 6 cm

adjustable opening in one wall, which was lined with grounded aluminum tubing connected to a hot water pump (NES Laboratories, Inc.) and served as a thermode. A standard rodent watering bottle containing room temperature sweetened condensed milk (diluted 1:2 with water) was mounted outside the cage. Unrestrained rats were placed individually into separate boxes and the data acquisition system was activated (DATAQ Instruments, Inc.). The reward bottle was positioned such that the rat could only access the spout while simultaneously contacting the thermodes on either side of its face. Contact of the rat's tongue with the metal spout on the water bottle completed an electrical circuit, and each spout contact was recorded as a "licking" event. A separate circuit was established from the metal thermode to the rat by grounding the floor with an aluminum sheet for recording of "facial contact" events. The duration of each facial contact and the total number of events (licking, facial contact) were recorded. Rats first completed baseline training at 37°C (N = 5 sessions). The total number of events was determined for both licking (reward) contacts and facial stimulus contacts, and the cumulative duration of facial stimulus contacts was also computed. Two pain indices were calculated by evaluating: (1) the ratio of the number of reward/facial contact events and (2) the duration per contact for the facial stimulus. With the thermode set at a noxious temperature, increases in both parameters are indicative of analgesia (5, 6). Data analyses were performed using custom-written routines (University of Florida) in LabVIEW Express (National Instruments Corporation) and Excel (Microsoft).

References

1. Roh EJ, Keller JM, Olah Z, Iadarola MJ, and Jacobson KA. Structure-activity relationships of 1,4-dihydropyridines that act as enhancers of the vanilloid receptor 1 (TRPV1). *Bioorg Med Chem.* 2008;16(20):9349-58.

2. Karai LJ, Russell JT, Iadarola MJ, and Olah Z. Vanilloid receptor 1 regulates multiple calcium compartments and contributes to Ca2+-induced Ca2+ release in sensory neurons. *J Biol Chem.* 2004;279(16):16377-87.
3. Christensen SM, Dillon LA, Carvalho LP, Passos S, Novais FO, Hughitt VK, Beiting DP, Carvalho EM, Scott P, El-Sayed NM, et al. Meta-transcriptome Profiling of the Human-Leishmania braziliensis Cutaneous Lesion. *PLoS Negl Trop Dis.* 2016;10(9):e0004992.
4. Green BB, Houseman EA, Johnson KC, Guerin DJ, Armstrong DA, Christensen BC, and Marsit CJ. Hydroxymethylation is uniquely distributed within term placenta, and is associated with gene expression. *FASEB J.* 2016;30(8):2874-84.
5. Neubert JK, Widmer CG, Malphurs W, Rossi HL, Vierck CJ, Jr., and Caudle RM. Use of a novel thermal operant behavioral assay for characterization of orofacial pain sensitivity. *Pain.* 2005;116(3):386-95.
6. Neubert JK, Rossi HL, Malphurs W, Vierck CJ, Jr., and Caudle RM. Differentiation between capsaicin-induced allodynia and hyperalgesia using a thermal operant assay. *Behav Brain Res.* 2006;170(2):308-15.
7. Anderson EM, Mills R, Nolan TA, Jenkins AC, Mustafa G, Lloyd C, Caudle RM, and Neubert JK. Use of the Operant Orofacial Pain Assessment Device (OPAD) to measure changes in nociceptive behavior. *J Vis Exp.* 201376):e50336.
8. Karai L, Brown DC, Mannes AJ, Connelly ST, Brown J, Gandal M, Wellisch OM, Neubert JK, Olah Z, and Iadarola MJ. Deletion of vanilloid receptor 1-expressing primary afferent neurons for pain control. *J Clin Invest.* 2004;113(9):1344-52.
9. Neubert JK, Maidment NT, Matsuka Y, Adelson DW, Kruger L, and Spigelman I. Inflammation-induced changes in primary afferent-evoked release of substance P within trigeminal ganglia in vivo. *Brain Res.* 2000;871(2):181-91.
10. Chiu IM, Barrett LB, Williams EK, Strochlic DE, Lee S, Weyer AD, Lou S, Bryman GS, Roberson DP, Ghasemlou N, et al. Transcriptional profiling at whole population and single cell levels reveals somatosensory neuron molecular diversity. *Elife.* 2014;3(
11. Sapio MR, Goswami SC, Gross JR, Mannes AJ, and Iadarola MJ. Transcriptomic analyses of genes and tissues in inherited sensory neuropathies. *Exp Neurol.* 2016;283(Pt A):375-95.
12. Goswami SC, Mishra SK, Maric D, Kaszas K, Gonnella GL, Clokie SJ, Kominsky HD, Gross JR, Keller JM, Mannes AJ, et al. Molecular signatures of mouse TRPV1-lineage neurons revealed by RNA-Seq transcriptome analysis. *J Pain.* 2014;15(12):1338-59.
13. Carroll SL, Silos-Santiago I, Frese SE, Ruit KG, Milbrandt J, and Snider WD. Dorsal root ganglion neurons expressing trk are selectively sensitive to NGF deprivation in utero. *Neuron.* 1992;9(4):779-88.
14. Murphy NP, Mills RH, Caudle RM, and Neubert JK. Operant assays for assessing pain in preclinical rodent models: highlights from an orofacial assay. *Curr Top Behav Neurosci.* 2014;20(121-45.

Supplemental Table 1 – Demographics of canine subjects and clinical care during RTX injection procedure.

Dog	Sex	Breed	Age (years)	Body weight (kg)	Premedication	Induction	Anesthesia Time* (minutes)	Rectal Temperature at Extubation	Additional Medications During Recovery**
1	M	Rottweiler	8	38	Hydromorphone 7.5 mg Acepromazine 0.75 mg	Ketamine 110 mg Diazepam 11 mg	90	98.7	Acepromazine 0.1 mg
2	F	Labrador Retriever	9	48	Hydromorphone 5 mg Acepromazine 0.94 mg	Ketamine 142 mg Diazepam 14.1mg	75	97.9	Dexmedetomidine 48mg Acepromazine 0.1mg Methadone 5mg Flumazenil 0.9mg
3	M	Greyhound	8	44	Methadone 11 mg Acepromazine 0.44 mg	Ketamine 132 mg Diazepam 13.2 mg	180	100.1	Methadone 4.4 mg Acepromazine 1mg
4	F	Great Dane	9	50	Hydromorphone 5 mg Acepromazine 0.25mg	Ketamine 250 mg Diazepam 12.5 mg Propofol 80 mg	90	97.2	None
5	F	Labrador Retriever	9	39	Methadone 5 mg Acepromazine 0.4 mg	Ketamine 195 mg Diazepam 9.8 mg Methadone 2 mg	110	98.1	Flumazenil 0.5mg Acepromazine 0.2 mg
6	F	Mixed Breed	13	35	*No procedure*	-	-	-	-
7	M	Golden Retriever	10	46	*No procedure*	-	-	-	-
8	F	Mixed Breed	9	42	*No procedure*	-	-	-	-
9	M	Bullmastiff	8	81	*No procedure*	-	-	-	-
10	M	Labrador Retriever	10	32	*No procedure*	-	-	-	-
11	F	Labrador Retreiver	7	50	*No procedure*	-	-	-	-

*Intubation to extubation

** Post RTX injection to ambulatory discharge from the recovery room

Supplemental Table 2 – Neurological assessment of resiniferatoxin (RTX) treated canine subjects. Male and female canine subjects (beagles) were assessed in an independent GLP laboratory as part of an IND application for the usage of intrathecal RTX in humans. The maximum tolerated dose (3.6 µg/kg) as well as a small number of dogs at higher dose tiers were examined on a variety of parameters. Mental status, gait, and postural reactions were observed as part of a standard neurologic evaluation. Only one incident of abnormality was observed in one male canine treated with 3.6 µg/kg RTX. This reaction, however, was also observed before dosing with RTX, indicating this was not related to treatment.

				Gait		Postural reactions		
	Group	N	Mental status	Visual	Motor	Proprioceptive positioning	Wheelbarrow	Hemistanding
Control	male	4	Normal (4/4)	Yes (4/4)	Normal (4/4)	Normal (4/4)	Normal (4/4)	Normal (4/4)
	female	4	Normal (4/4)	Yes (4/4)	Normal (4/4)	Normal (4/4)	Normal (4/4)	Normal (4/4)
1.2 µg/kg	male	4	Normal (4/4)	Yes (4/4)	Normal (4/4)	Normal (4/4)	Normal (4/4)	Normal (4/4)
	female	4	Normal (4/4)	Yes (4/4)	Normal (4/4)	Normal (4/4)	Normal (4/4)	Normal (4/4)
3.6 µg/kg	male	6	Normal (6/6)	Yes (6/6)	Normal (5/6)*	Normal (6/6)	Normal (6/6)	Normal (6/6)
	female	4	Normal (4/4)	Yes (4/4)	Normal (4/4)	Normal (4/4)	Normal (4/4)	Normal (4/4)
12 µg/kg	female	2	Normal (2/2)	Yes (2/2)	Normal (2/2)	Normal (2/2)	Normal (2/2)	Normal (2/2)
36 µg/kg	male	1	Normal (1/1)	Yes (1/1)	Normal (1/1)	Normal (1/1)	Normal (1/1)	Normal (1/1)

*One animal judged "slightly paralytic" at both pre-dose and study day 15

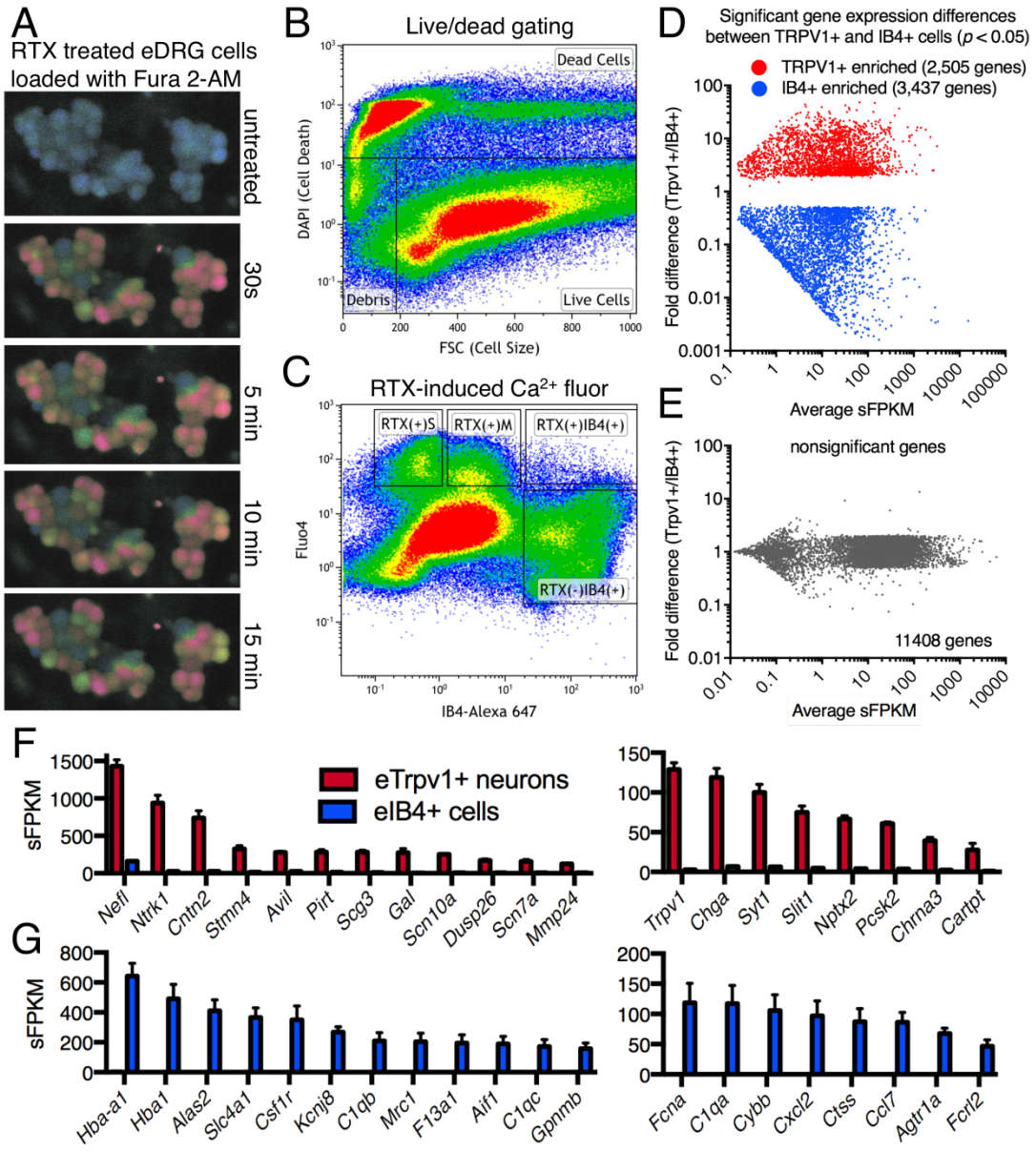

Supplemental Figure 1 – Fluorescence-activated cell sorting of TRPV1+ neurons using stimulation of embryonic DRGs (eDRGs) with resiniferatoxin (RTX). Cells were loaded with calcium sensitive dyes (see methods) and stimulated with RTX. The fluorescent signal after RTX-induced calcium influx is detectable by 30s, and lasts at least 15 minutes (A, single experiment). This RTX-sensitive signal was used for cell-sorting. Dissociated cells were sorted for live vs. dead cells using DAPI (B) and live cells were passed through a second gate based on RTX-induced calcium influx and IB4 fluorescence (C). RTX responsive cells were subdivided by size into small and medium populations. After sorting, cells were sequenced, and differential expression was tabulated for RTX-responsive small cells (TRPV1+) vs. IB4+ cells (D, E). Differential genes were identified by Wilcoxon Mann-Whitney testing in MAGIC, and representative highly expressed marker genes are shown for both the eTRPV1+ (F), and the eIB4+ (G) populations (B-F, n = 4 sort experiments). In total, 2,505 transcripts were enriched in the

eTRPV1 population and 3,437 genes were enriched in the eIB4+ population ($p<0.05$)(D) while 11,408 transcripts were shared by these populations (E). In contrast to a previous dataset using microarray to characterize the adult IB4+ neuronal population (10), the present eIB4+ dataset contains mostly non-neural cells. While IB4 binding in the *adult* DRG is largely confined to a subpopulation of non-peptidergic unmyelinated sensory neurons, in the embryonic tissue it also binds to several other cell types, including endothelial cells. Examples of highly expressed marker genes for each population are shown (F, G). The eTRPV1+ population is highly enriched for *Trpv1*, as well as several voltage-gated sodium channel genes, and other markers of nociceptive neuronal progenitors (F). Because of its embryonic status, the eIB4+ population contains many markers of blood and vasculature such as the hemoglobin genes, and the vascular K+ channel *Kcnj8* (G). Raw sequencing data are available for this dataset via the Sequence Read Archive database under BioProject# PRJNA428250.

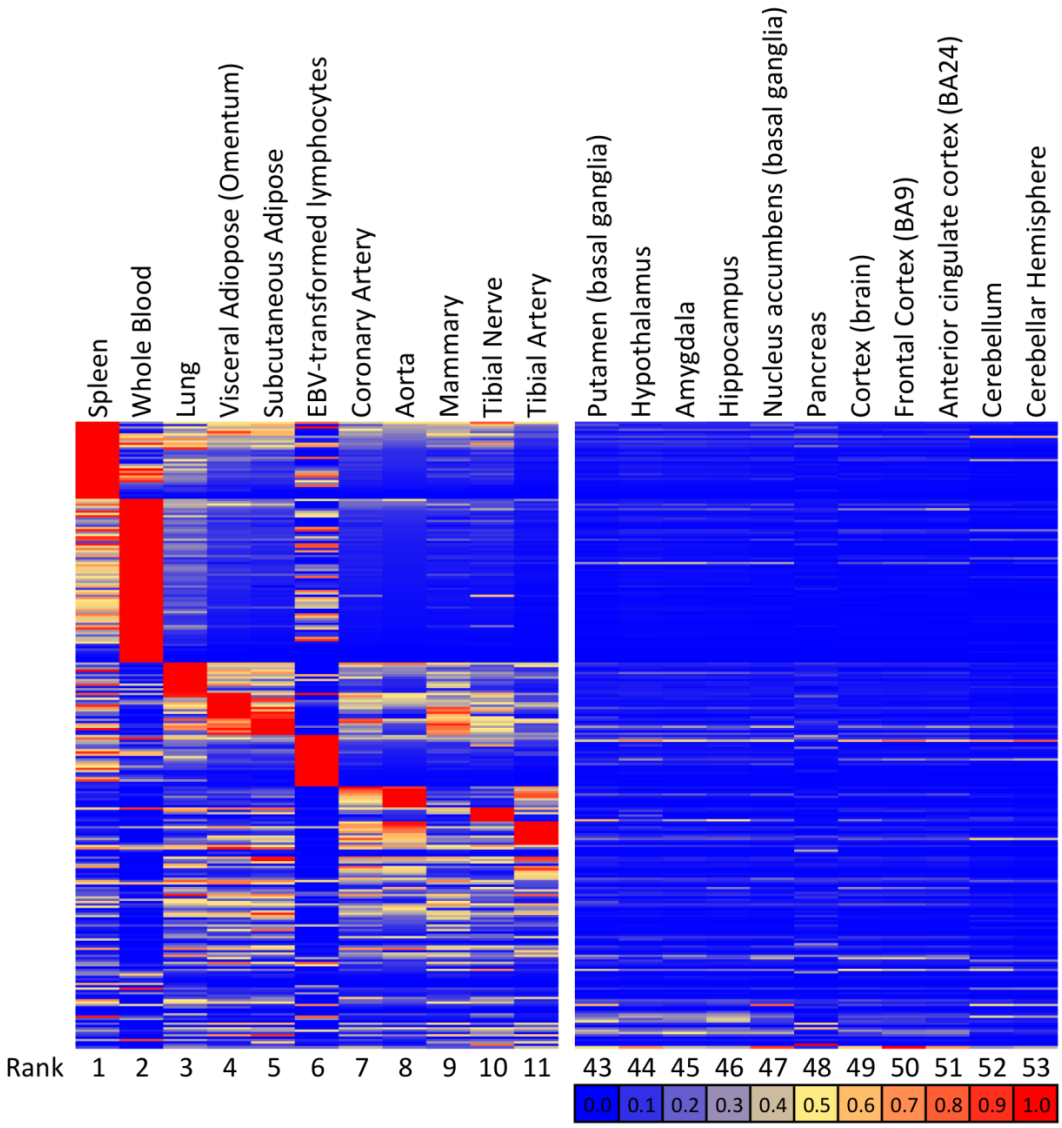

Supplemental Figure 2 – Highest differentially expressed genes in eIB4+ relative to TRPV1+ sorted embryonic DRG cells in GTEx tissue expression atlas. The most highly differential genes in the eIB4+ subpopulation compared to the eTRPV1 population were mapped for tissue expression in the adult human using the GTEx median RPKM values. Each tissue from the full dataset of 53 samples were ranked for enrichment, and the 11 most enriched, and 11 least enriched are plotted. Among the highest enriched tissues are spleen and blood, which likely reflects the presence of circulating blood cells in the eIB4+ population. Brain regions are among the tissues lowest in eIB4+ genes, indicating that these cells do not exhibit a neural gene expression profile, and indicating that they are most likely non-neural.

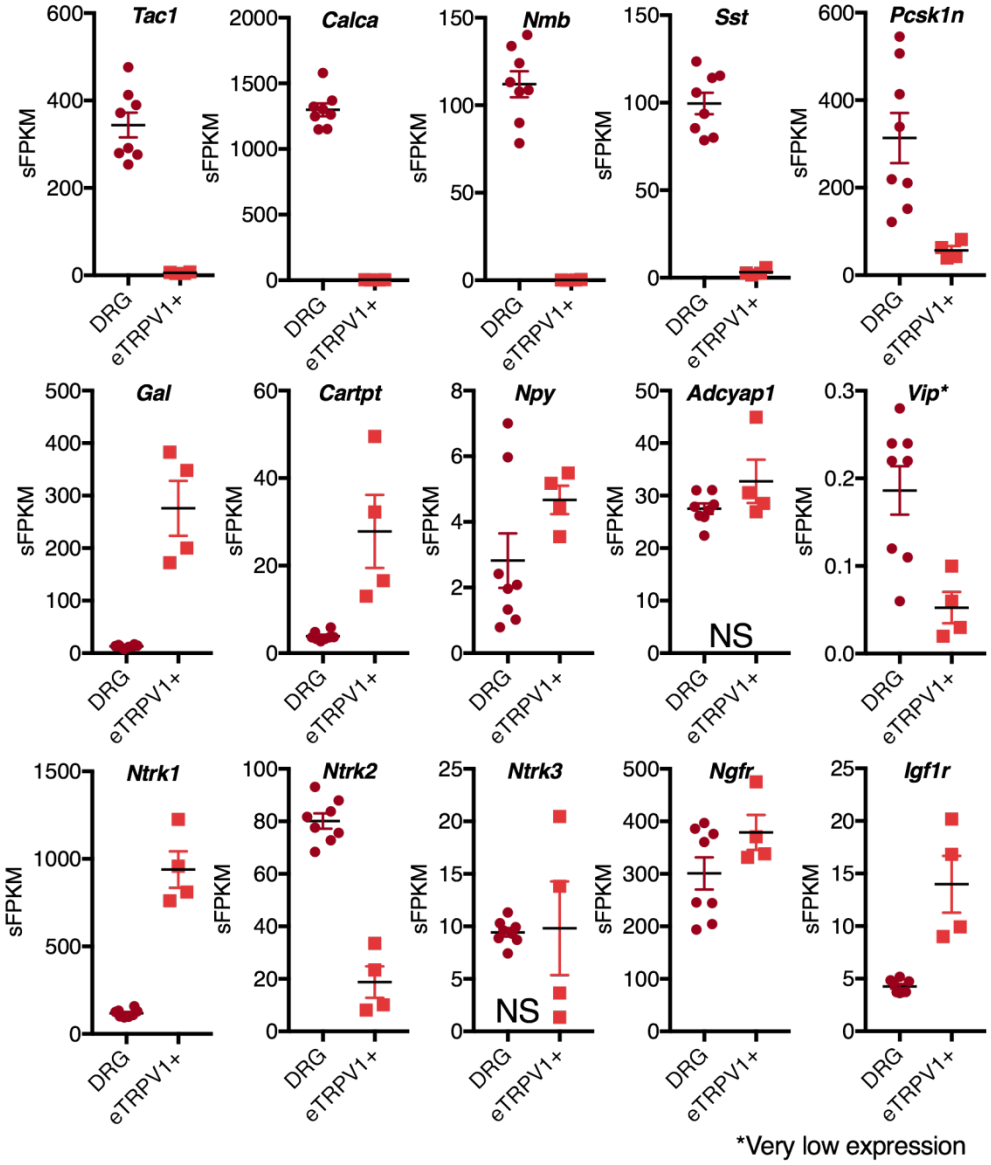

Supplemental Figure 3. Panel of differentially expressed genes between whole DRG homogenate and embryonic TRPV1+ neurons after cell sorting (eTRPV1+). Transcripts from eTRPV1+ neurons were sequenced (n = 4) and analyzed using the MAGIC RNA-Seq pipeline, and compared to a previously published whole DRG dataset (n = 8)(11) using Wilcoxon Mann-Whitney testing. Embryonic TRPV1+ neurons have low levels of several neuropeptides (*Tac1*, *Calca*, *Nmb*, *Sst*, *Pcsk1n*) but higher levels of expression of Galanin (*Gal*), CART peptide (*Cartpt*) and neuropeptide Y (*Npy*) precursor transcripts. They have roughly equivalent levels of adenylate cyclase activating polypeptide (*Adcyap*) transcript to DRG homogenate. These cells are characterized by their high level of TrkA receptor expression (*Ntrk1*) with low levels of TrkB (*Ntrk2*) and TrkC (*Ntrk3*). Genes are significantly differential except where noted. The e16.5 TRPV1 neurons express very low levels of mRNAs encoding the neuropeptides that are abundantly expressed in the adult such as *Tac1*, *Calca*, *Nmb*, *Sst* and *Pcsk1n,* all of which are expressed in TRPV1 lineage neurons in the adult (12). In contrast to levels of

Substance P and CGRP precursor mRNAs, the eTRPV1 DRG neurons have high levels of *Cartpt, Gal*, and *Npy*. The eTRPV1 neurons also express very high levels of *Ntrk1*, which encodes TrkA, the receptor tyrosine kinase that binds NGF and is known to be required for the development of nociceptive neurons (13). All genes are significant ($p < 0.05$) except where noted. NS = not significant.

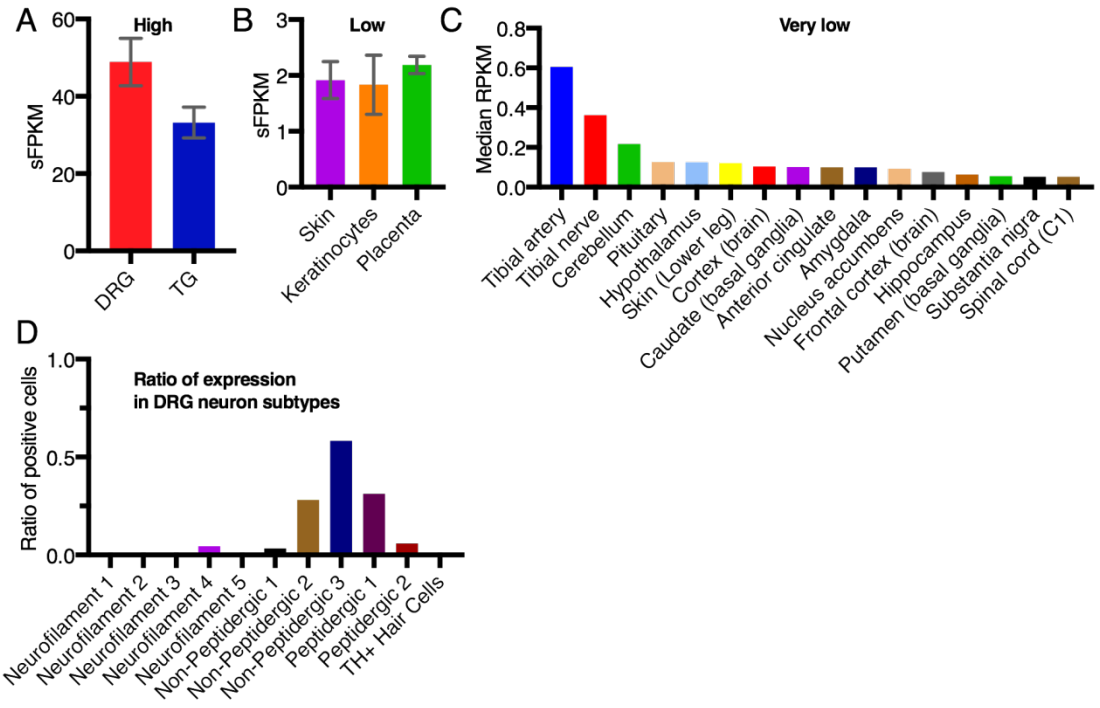

Supplemental Figure 4– TRPV1 expression from transcriptomic analyses. RNA-Seq expression data was mined for human *TRPV1* from several data sources. Dorsal root ganglia (DRG, n = 4) and trigeminal ganglia (TG, n = 5) datasets were analyzed using MAGIC, showing high expression in both of these sensory ganglia (A). FASTQ files were mined from the sequence read archive (SRA) database and reanalyzed using MAGIC for skin (n = 6), keratinocytes (n = 7), and placenta (n = 22)(B). In each of these tissues *TRPV1* expression is low, but detectable. Data analyzed using the MAGIC pipeline (sFPKM values) were quantified using Aceview annotations of the human genome. Median RPKM values for several tissues (C) were mined from the GTEx database, showing low but detectable expression in tibial artery and nerve, with very low expression in other tissues. Expression data from single cell sequencing of mouse DRG neurons was mined and plotted as a ratio of expression (D) using values presented in the original publication.

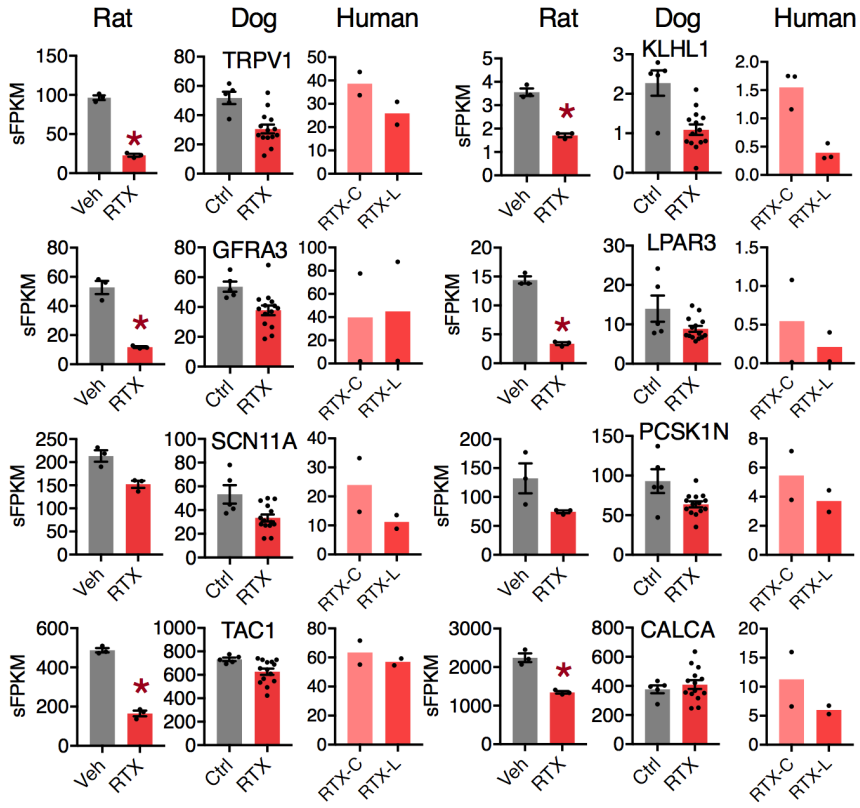

Supplemental figure 5. Selected genes from transcriptomic analyses of rat, dog, and human samples. Raw data with replicate values are plotted for several genes across the datasets. Several of the genes most highly altered by RTX treatment in either the rat in vitro studies (n = 3) or dog (n = 3 control, n = 5 treated) and human clinical samples (n = 1) are shown. Extra data points for dog and human samples show additional technical replicates from each ganglia. Levels of mRNA are quantified for the two major neuropeptide precursors expressed by nociceptors, TAC1 and CALCA, which code for the precursors to Substance P and CGRP respectively. The expression levels of several of these genes are reduced by the in vitro cell ablation study using RTX, but unaltered in the dog DRG after intrathecal resiniferatoxin. The *Tac1* gene is also unaltered between cervical and lumbar ganglia of the human patient treated with RTX intrathecally.

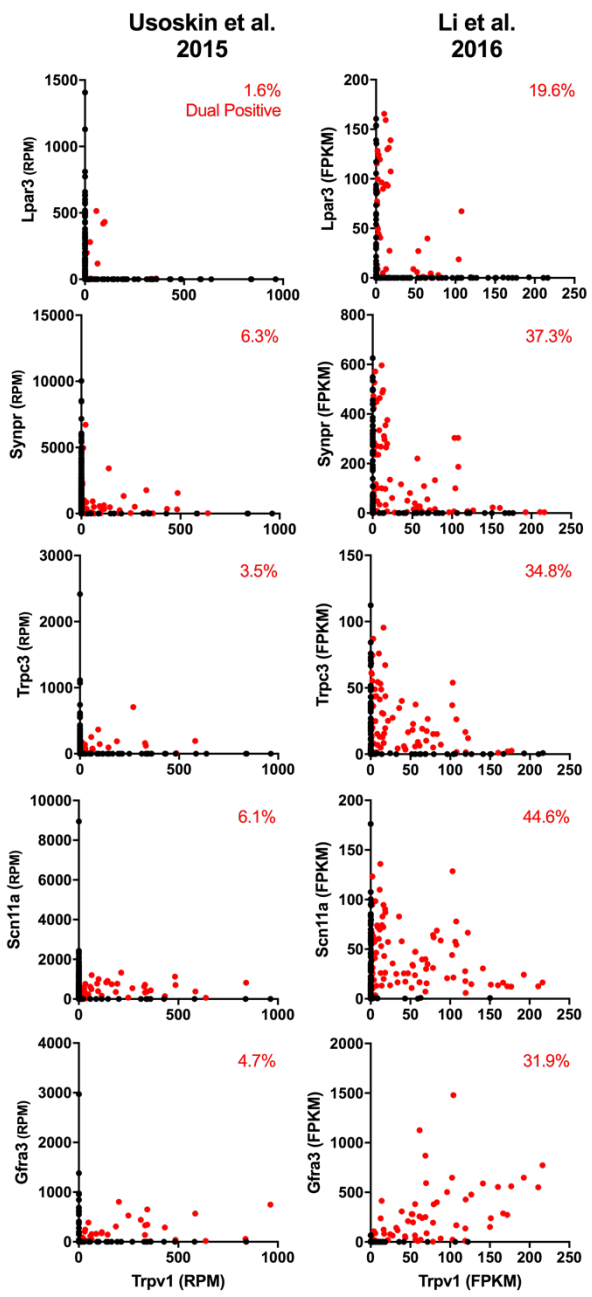

Supplemental Figure 6 - Relationship between *Trpv1* expression and select genes with decreased expression in the DRG after RTX treatment assessed by single-cell RNA sequencing. Data is from publicly available databases published by Usoskin et al. (2015) and Li et al. (2016). The database from Usoskin et al. expresses transcript counts in reads per million (RPM), and cells with >1 RPM for both plotted genes are shown in red. The database from Li et al. expresses transcript counts in fragments per kilobase of transcript per million mapped reads (FPKM), and cells with >1 FKPM for both plotted genes are shown in red. The percentage of cells analyzed that exceed this threshold is shown in the upper right of each panel. Of note, Li et al. had higher coverage with 10,950 detectable genes per neuron on average, whereas Usoskin et al. had 3,574 detectable genes per neuron on average.

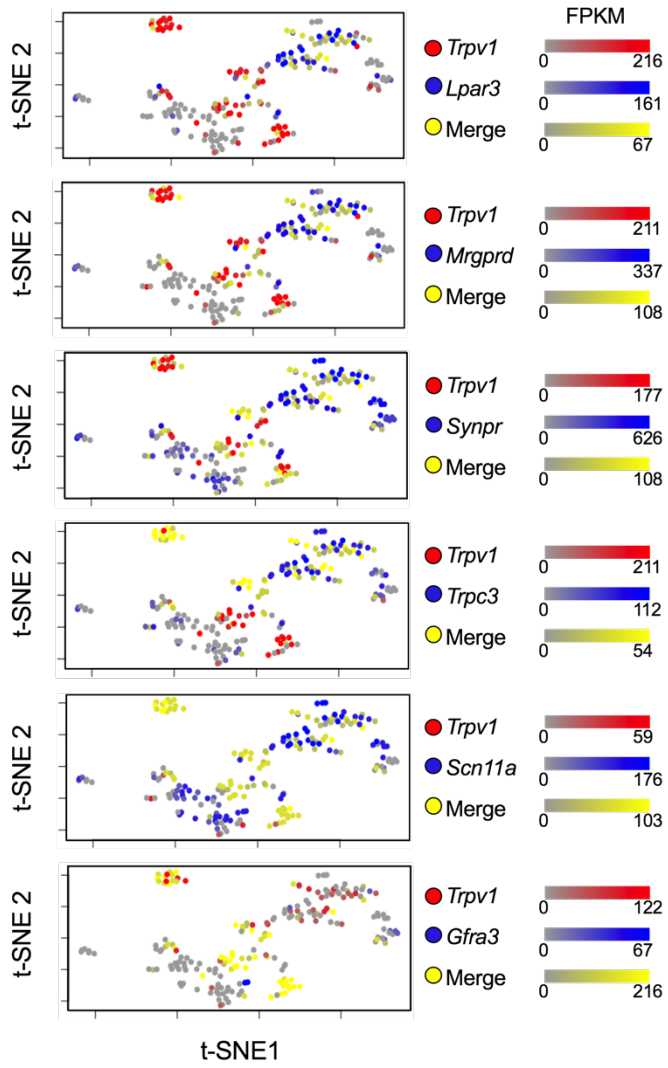

Supplemental Figure 7. Colocalization of *Trpv1* and select genes in the mouse DRG assessed by single-cell RNA sequencing. Data are from a publicly available database published by Li et al. (2016). Single cells in this database were visualized using the Barnes-Hut implementation of the t-Distributed Stochastic Neighbor Embedding (t-SNE) technique according to their gene expression profiles (van der Maatan, 2014). Cells with similar gene expression profiles are plotted near each other in the 2-dimensional embedding. Cells were colored based on the expression of select genes (shown in the legend to the right of each panel). Color scales were normalized separately for each transcript by the log-transformed range of each gene's expression. As can be seen in the visualization, all of these genes have some degree of coexpression in *Trpv1* expressing neurons. Plots were generated using the Rtsne package in R version 3.3.1 (Krijthe, 2015).

Reference to R package

Jesse H. Krijthe (2015). Rtsne: T-Distributed Stochastic Neighbor Embedding using a Barnes-Hut Implementation, URL: https://github.com/jkrijthe/Rtsne

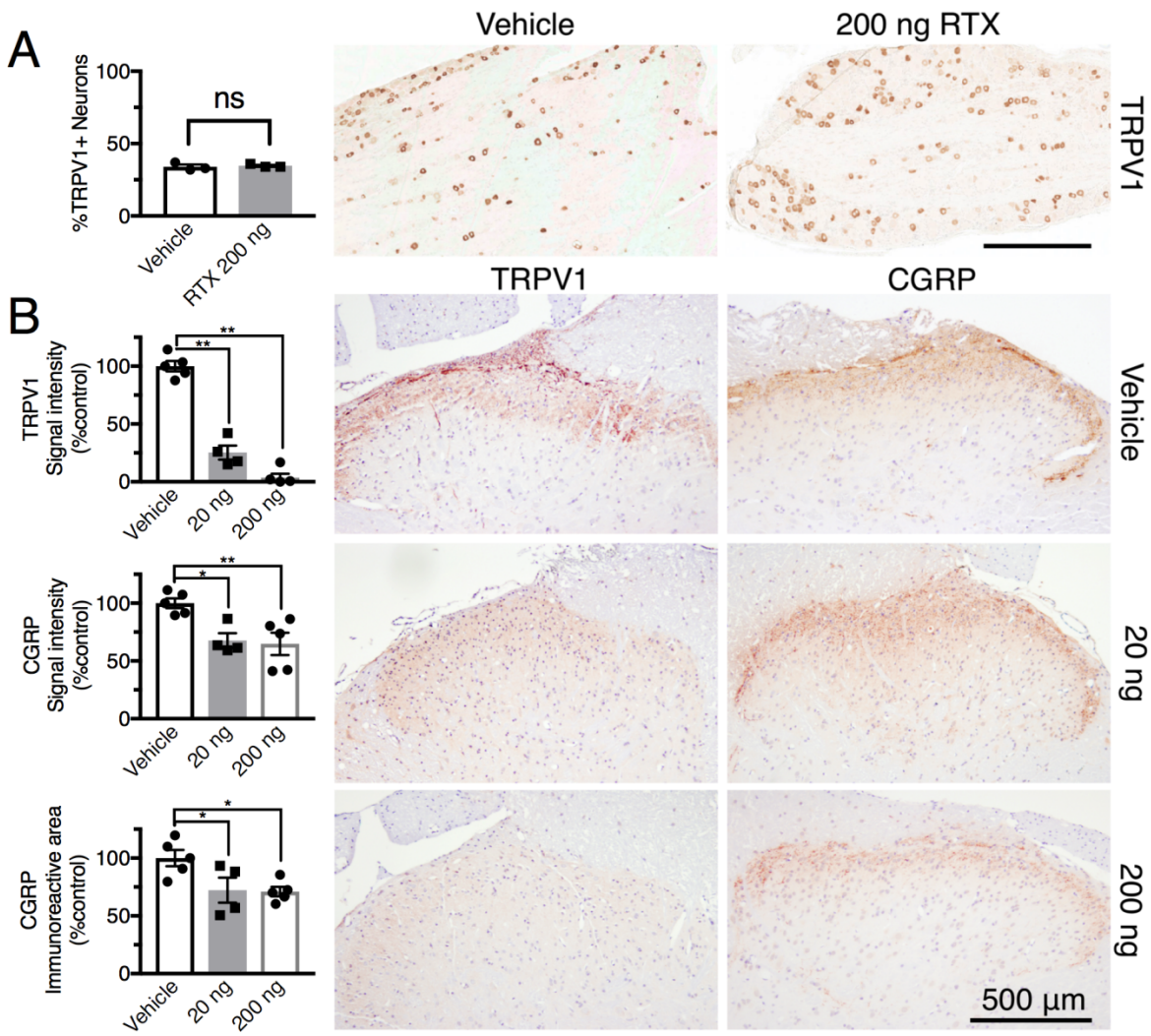

Supplemental Figure 8– Dose response to intrathecal resiniferatoxin treatment in rat. Lumbar intrathecal injections of vehicle or 200 ng RTX were performed in Sprague-Dawley rats, and TRPV1 immunoreactivity (1:1,000, ThermoFisher, PA1-748) was examined in the lumbar DRGs. No significant difference in the percentage of TRPV1+ neurons was observed, and the small densely positive cells were still observable after RTX treatment (A, n = 3). Several doses were explored to examine the effects of lumbar intrathecal injection of RTX on the dorsal spinal cord DRG projections. TRPV1 and CGRP staining were assessed in the lumbar enlargement of the dorsal spinal cord, with staining primarily detected in the superficial laminae. After RTX injection at 20 ng, staining for TRPV1 and CGRP was reduced, but still detectable. Virtually no TRPV1 was detectable after 200 ng intrathecal RTX, while CGRP was still detectable, reflecting the population of CGRP+ neurons that do not express TRPV1. Sections were counterstained with cresyl violet. $N \geq 4$ animals were examined. Color deconvolution and subsequent densitometry were performed in FIJI. One-way ANOVA was performed to compare each RTX dose to vehicle (*, $p \leq 0.05$; **, $p \leq 0.01$, $n \geq 4$).

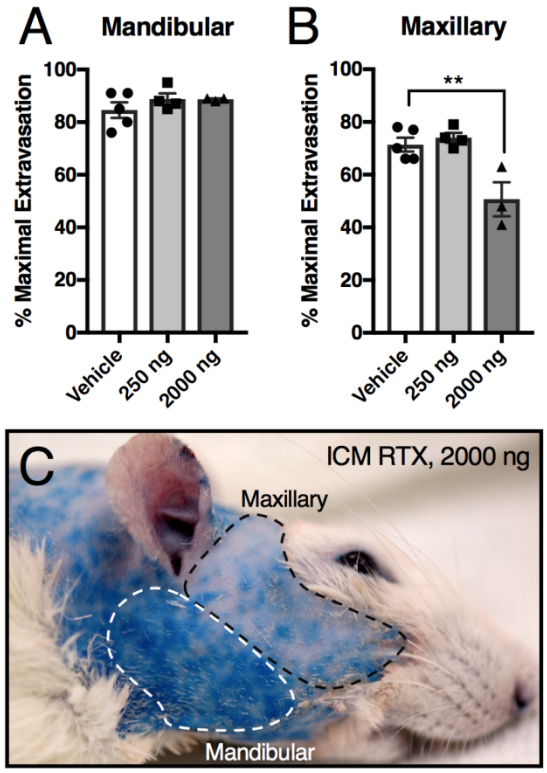

Supplemental Figure 9 - Densitometric measurement of extravasation in two trigeminally innervated facial regions after intracisternal resiniferatoxin (RTX). For each rat injected with Evans Blue dye, images were captured using a Nikon D50 with an AF-S VR Micro-Nikkor 105mm f/2.8G IF-ED lens (Nikon, Tokyo, Japan). Extravasation was examined by isolating the blue signal using image deconvolution in Fiji, and the brilliant blue deconvolution settings. Initial observations showed a possible decrease in extravasation after the 2000 ng RTX ICM dose in the area below the eye following the maxillary (V2) division of the trigeminal nerve. Sections of the images were quantitated in Fiji with care taken to avoid skin discontinuities and hairs. Measurements were taken in both the maxillary and mandibular regions of each rat, and averaged such that each point represents a single animal. No difference was observed between vehicle and 250 ng RTX animals (n = 5). In general, the maxillary region showed less extravasation than the mandibular. In 2000 ng RTX treated animals, the maxillary region was reduced to approximately 50% of maximal extravasation observed ($p < 0.01$, n = 3).

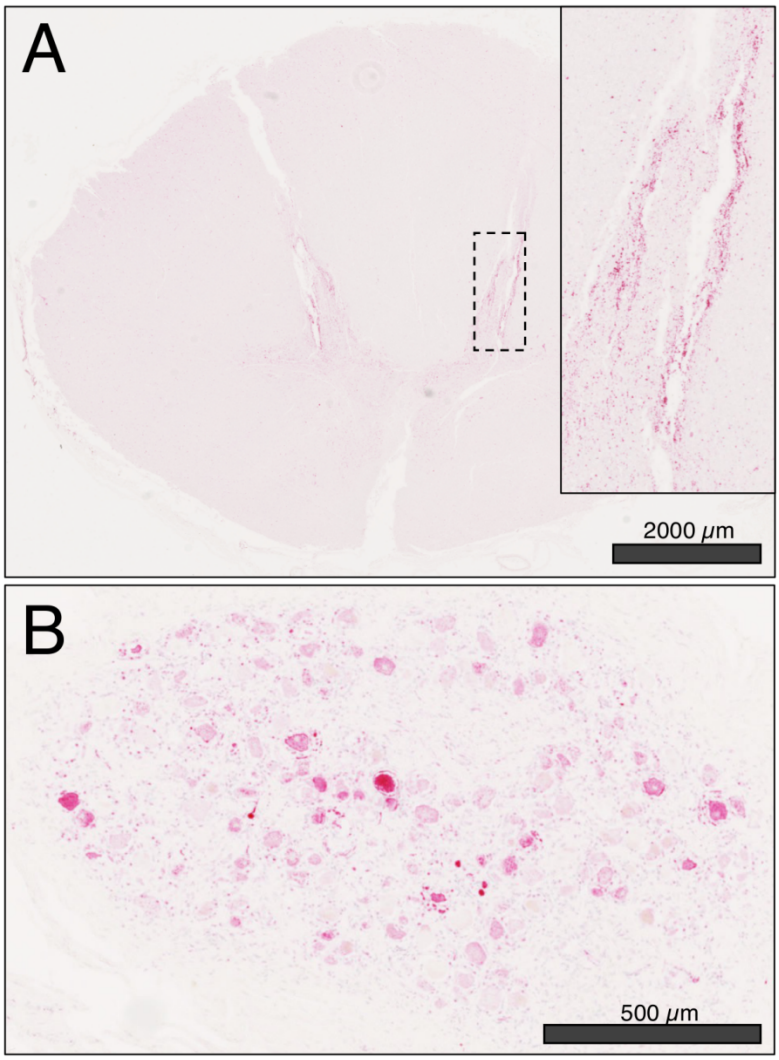

Supplemental Figure 10 – Detection of CGRP in RTX-treated human thoracic ganglia. Staining for primary afferent nociceptive markers was difficult to detect in the dorsal horn of the RTX treated human patient. A stain of the n = 1 patient spinal cord and DRG using longer development shows that it is possible to detect a CGRP signal in both tissues. (A) In the uppermost thoracic sections examined (approximately T6), CGRP was detectable in the dorsal horn. (B) Matched DRG sections stained densely for CGRP.

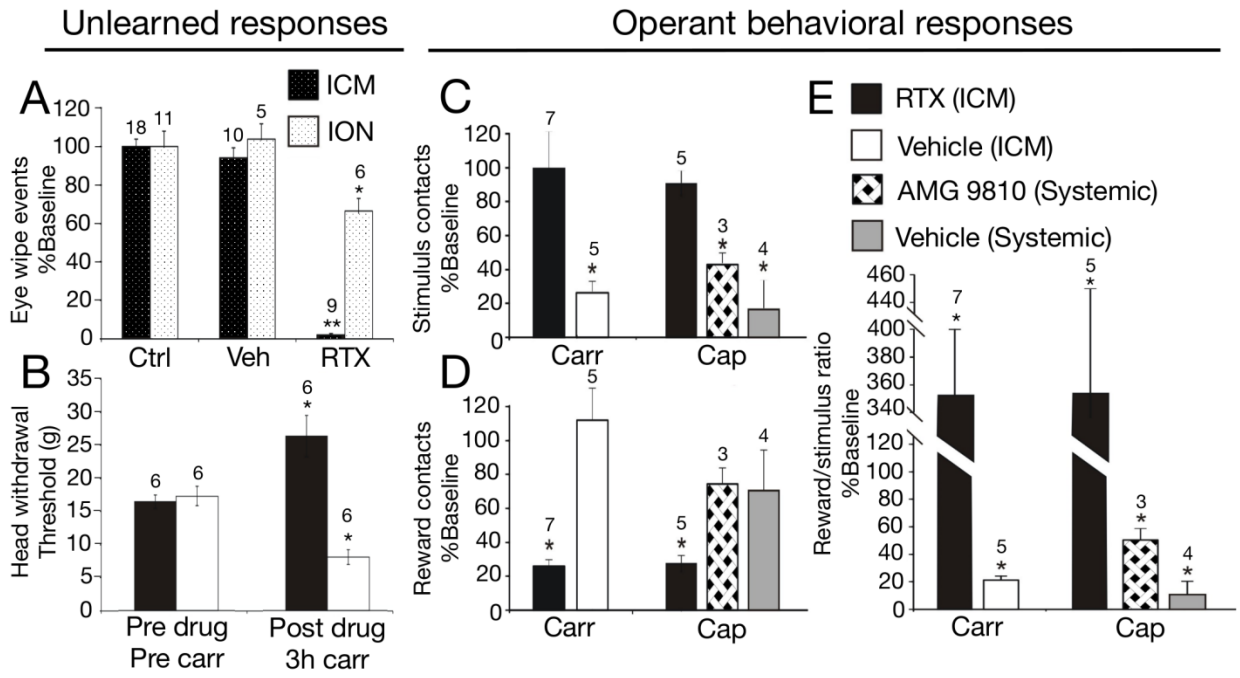

Supplemental Figure 11 - RTX inhibits nociceptive unlearned and learned operant behavioral responses. Rats were injected intrathecally (ICM) or infraorbitally (ION) with vehicle or RTX (A) and capsaicin (0.1%, 25 μl) was placed directly onto the cornea of the eye to measure unlearned nociceptive responses (number of eye wipes over 1 minute). Untreated rats did not differ from vehicle (A), while RTX injection (250 ng) significantly decreased wipes in both injection paradigms, with near total abolition of responses in the ICM route (A). Von Frey testing was completed before and after carrageenan inflammation of the face (3 hours post inflammation) in rats pretreated with ICM RTX (250 ng) or vehicle 1 week prior (B). Rats treated with RTX demonstrated a significant block of inflammation-induced mechanical hyperalgesia. Vehicle-treated rats showed a significant reduction of force (increased hyperalgesia) needed to elicit a head withdrawal response following inflammation. Intracisternal RTX was also evaluated for efficacy for reversing inflammatory hyperalgesia in rats by assessment of operant behavioral responses (C-E). Thermal hyperalgesia was induced by injection of carrageenan or capsaicin. Briefly, rats were trained to lick for a sweetened condensed milk reward, which the rat could obtain only while contacting a 48°C thermode. RTX increased licking contact events (C), which are events in which the rat licks for reward while in contact with the thermode. Simultaneously, it decreased facial contact events in general, indicating that the RTX treated rats made contact with the thermode fewer times (D). In general, the ratio of rewarded sessions to attempted sessions is higher in RTX-treated rats (E). RTX treatment did not alter overall reward licking events during the test session, indicating a change in strategy where there are longer, more reward-obtaining licking sessions while in contact with the 48°C thermode, but not an overall change in consumption of food reward. This indicates a higher tolerance for thermal stimulation in RTX treated rats with both carrageenan and capsaicin-induced thermal hyperalgesia. Systemic administration (intraperitoneal) of the TRPV1 antagonist (AMG 9810) partially inhibited the capsaicin-induced hyperalgesia. For the capsaicin eye-wipe response, a general linear model multivariate analysis was used to assess the effects of ICM

treatment (baseline, vehicle, RTX) and treatment site (ICM vs. ION) (A). Mechanical sensitivity was assessed either within a treatment (pre- vs. post-inflammation) or between treatments (RTX vs. vehicle) at baseline and post-inflammation time points using a paired T-test (B). For the operant outcomes (C-E), an ANOVA was used to evaluate the effects of treatment on each outcome measure following topical capsaicin application and when significant differences were found, post-hoc comparisons were made using the Tukey HSD. A two-tailed Student's T-test was used to evaluate the effects of treatment on carrageenan-induced inflammatory pain. Numbers above each bar show the number of rats in that group, *, $p<0.05$; **, $p<0.001$.

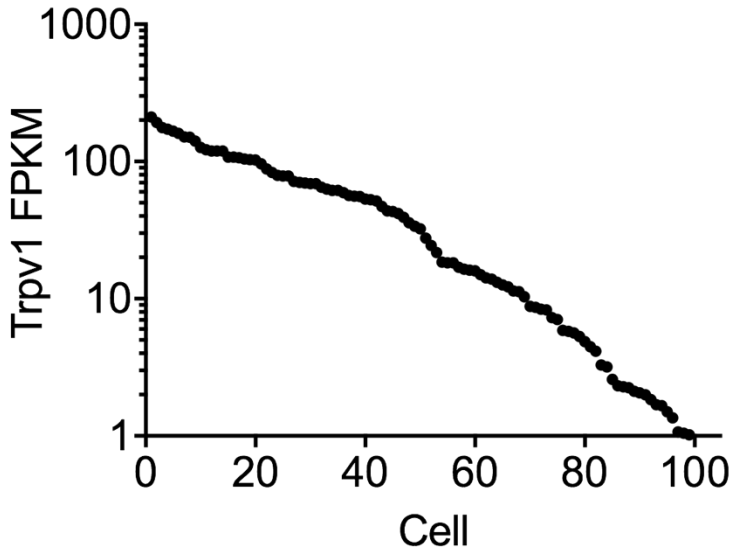

Supplemental Figure 12. The range of *Trpv1* expression in mouse DRG assessed by single-cell RNA sequencing. Single-cell expression data were mined from Li et al (2016) and cells expressing *Trpv1* above 1 FPKM were extracted and sorted in descending order based on expression level. Note that 44 cells with *Trpv1* expression below 1 FPKM are not plotted. While FPKM values of single-cell sequencing must be interpreted with caution due to low precision, there is a wide range of *Trpv1* expression, with 21/99 cells expressing *Trpv1* between 1 FPKM and 10 FPKM, while cells in the upper range express *Trpv1* above 100 FPKM.